Solidification kinetics of $Fe_{0.5}Pt_{0.5}$ clusters in an Ar carrier gas: Molecular dynamics simulations

N. Lümmen[1] and T. Kraska[2]
[1]*Department of Physics and Technology, University in Bergen, Postboks 7800, 5020 Bergen, Norway*
[2]*Physical Chemistry, University of Cologne, D-50939 Cologne, Germany*
(Received 2 February 2007; revised manuscript received 20 September 2007; published 25 January 2008)

Small clusters exhibit different behaviors in many physical properties compared to bulk systems. A long-standing problem in cluster science is the question how small clusters solidify. Here, we analyze the solidification of small $Fe_{0.5}Pt_{0.5}$ clusters by molecular dynamics simulation. We use a carrier gas thermostat in the simulations to mimic the experiment rather than an idealized ensemble. This enables us to explore the solidification process under more realistic conditions. We find that structure formation starts below the surface layers and spreads quickly throughout the cluster. We observe apparent negative thermal expansion and apparent negative heat capacity. These effects and the related solidlike-liquidlike dynamic coexistence are explained kinetically by means of the short duration of cluster solidification in connection with a slow heat removal.

DOI: 10.1103/PhysRevB.77.045425 PACS number(s): 61.46.Bc, 36.40.Ei, 64.70.D−, 31.15.xv

I. INTRODUCTION

Metal nanoparticles with new size dependent thermodynamic, electronic, and optical properties are promising building blocks for new materials. They can be employed as filling material to alter mechanical properties[1] for the development of catalysts for direct methanol fuel cells[2] or for high density magnetic storage[3] to mention only a few examples. Since the specific properties of the particles depend not only on their size but also on their structure and morphology, the understanding of the formation process is mandatory for the design of a selective production process. In addition, the morphology and atomic structure depend on the kinetics of the growth process. Similar to the effect of the nanometer size on the particle properties, the dynamics of particle formation, growth, and also structure formation is influenced by particle size. During growth, atomic structures can appear that are not stable in macroscopic atomic crystals. As an example, the icosahedral structure may be mentioned, which has a fivefold symmetry and is not capable of forming translation symmetry. Furthermore, phase transitions on the nanometer scale are not sharp but rather continuous. The solidlike and the liquidlike states can both be stable in a certain temperature range. In sufficiently small clusters, it is not possible to have the two phases at the same time like in bulk systems. The complete cluster switches from a solidlike to a liquidlike state. This effect can lead to a counterintuitive behavior such as the apparent negative heat capacity, which is an increase in temperature during heat removal. Such behavior has been found experimentally for small clusters,[4] in theoretical analysis,[5,6] and in molecular dynamics simulations of pure metal clusters such as sodium clusters[7] and copper clusters.[8] From a technological perspective, dynamic phase coexistence of nanoparticles and smaller clusters is of interest for nanophotonic switching devices.[9] This is because the optical properties of nanoparticles change from one phase state to the other.

The discussion of dynamically coexisting nanoparticles is often restricted to the melting process which is dominated by surface melting in the case of small nanoparticles.[9] Here, we investigate the second part of dynamic coexistence, the solidification of small clusters. Intuitively, a nucleation of the solidlike state in the cluster surface might be expected because the heat is removed from the cluster surface. The surface should cool down faster and hence solidification should start there. However, taking into account the effect of surface melting may suggest that a cluster does not start to solidify in the surface. It would rather lead to a solidlike core with a liquidlike surface. On the other hand, melting and solidification are not symmetric. Based on molecular dynamics (MD) simulations of the solidification of NiAl clusters, an influence of surface segregation on solidification has been proposed.[10] In that work, either solid nucleation was suppressed in the investigated time frame, depending on the composition of the cluster, or the formation of amorphous clusters was observed. In Monte Carlo (MC) simulations of pure gold clusters, solidification nucleation has been observed in the cluster surface.[11] MC simulations are somewhat complementary to MD simulations. With MC simulations, it is possible to cross high energetic barriers toward stable states. In MD, one may not reach the final state in given time but one can study the kinetic details including the formation of metastable states.

Clusters that completely switch back and forth between the liquidlike and the solidlike state, as mentioned above, exhibit the so-called dynamic phase coexistence rather than static coexistence. In several investigations of this phenomenon, dynamic[4–6] as well as static coexistence[12–15] have been found for nanometer sized pure metal clusters. Hendy[16] suggests an expression for a critical cluster radius that separates cluster sizes with dynamic and static coexistence. In the case of lead, he found dynamic coexistence for a 931 atom cluster, while a 1427 atom cluster exhibits static coexistence. However, the detailed mechanism of the solidification of metal clusters with dynamic coexistence in a carrier gas has not yet been investigated nor has the solidification of binary clusters been analyzed so far. In contrast to most investigations in this area, we do not use a microcanonical or a canonical ensemble but cool down the clusters by collisions with a carrier gas mimicking the experimental situation.[17,18] We think that this approach is more suitable to describe the real situation because nonequilibrium effects are inherently included. We chose the FePt system with clusters of 864 and

 ©2008 The American Physical Society

1123 atoms (diameters of 2.9 and 3.2 nm) and a mole fraction exactly or very close to 0.5. The understanding of the structure formation in this system, where the solidification analyzed here is only one step, is of great technological importance.[19] Furthermore, we investigate clusters that have been obtained from a vapor phase nucleation simulation[20] rather than perfectly ordered magic number clusters. For the understanding of the solidification process, we use here a shell by shell analysis of the temperature and the atomic order. We observe fast solidification with a nucleus below the surface of the clusters rather than in the surface. The solidification from the cluster core is explained by geometrical arguments. Apparent negative heat capacity as well as related apparent negative thermal expansion coefficients are observed. These effects are caused by the fact that coexisting phases in the cluster are not present for sufficient time in the clusters studied here. As a consequence, the latent heat cannot be removed instantaneously from the clusters by the carrier gas.

II. METHOD

Molecular dynamics simulation, which is the numerical solution of the equations of motion of each atom in the force field of all other atoms, has been performed using a cubic box. The equations of motion are calculated by a velocity-Verlet integrator with a time step of 1 fs. Standard techniques such as periodic boundary conditions, minimum image convention, and neighbor lists are used. Details of the method can be found in recent papers.[20,21] The interactions between the metal atoms are modeled by the embedded atom method (EAM),[20,22,23] while for argon, which serves as carrier gas, and for the metal-argon interaction, the Lennard-Jones potential is used. The EAM potential is an efficient model suitable for large systems and long simulation runs. The parametrization used here includes the interaction with the third next neighbors. It is correlated to experimental data and therefore reproduces all these properties, whereas specific properties such as magnetism cannot be extracted explicitly. The potential model stabilizes the binary ordered $L1_0$ phase in an equimolar cluster below 1100 K.[24] Simulations with this potential have shown that as the temperature is increased, the cluster loses the $L1_0$ structure and then eventually melts.[24] Although it is known that magnetism has an influence on the phase diagram of the FePt system,[25] it has no effect on the investigation here. According to the Ostwald step rule[26] in nonequilibrium, nonsteady state systems, the state with the closest free energy is formed first and not the most stable state. Therefore, on the time scale of the nonequilibrium simulation here, the disordered fcc phase is expected rather than the ordered $L1_0$ phase. This applies even at temperatures where the $L1_0$ phase is stable at equilibrium conditions. Hence, it is of interest to find out whether this is actually the case for this system or whether binary order appears during solidification. Furthermore, other special features of the FePt phase diagram existing at mole fractions much apart to the 1:1 mixture[25,27] are not relevant here because this investigation is restricted to equimolar systems. The carrier gas atoms are thermalized by velocity scaling, while the metal clusters are thermalized only by collisions with the argon atoms. There are three times as many carrier gas atoms (argon) as metal atoms in the system. For the determination of the structure, the common neighbor analysis (CNA) is employed.[24,28–30] This method has been used before, for example, to study structural changes in the melting of clusters[31] and cluster collision processes[21] but not yet for each shell of a cluster separately. The atoms in the surface are detected by the cone algorithm.[32] The second shell is identified by applying the cone algorithm after the surface atoms are removed. By repeating this procedure, the affiliation of all atoms to the different shells is obtained.

III. RESULTS

Clusters of different sizes and compositions are obtained from particle formation simulations.[20] To bring these clusters back into the liquidlike state first, they are heated up by setting the carrier gas temperature to 1600 K. For studying the cluster solidification, the carrier gas temperature is then decreased in 100 K steps every 4 ns, which leads to a cluster cooling rate of about 23.3 K/ns. At a carrier gas temperature of 1100 K, the investigated liquid-solid transition takes place. The experimental bulk solidus curve is at 1853 K for a mole fraction of one-half.[33,34] Based on a comparison of grain sizes in FePt films,[35] an estimation of the cluster melting temperature for the cluster sizes investigated here gives a value 25% below the experimental bulk melting temperature. However, this is a crude estimate since it is based on calculations with the Lennard-Jones potential for the metals.[35] The resulting melting temperature is 1390 K. Experimentally, bulk metal alloys can be undercooled by 20%,[36] which would give a temperature of about 1110 K in our case. From repeated melting and solidification simulations,[37] we obtain a reproducible temperature jump from 1430 to 1350 K at melting and from 1110 to 1300 K at solidification. The equilibrium melting temperature of the cluster is hence between 1110 and 1430 K consistently with the rough estimate above.

The solidification of the FePt clusters can be traced by the amount of local order in the clusters and by the temperature development. The solidification of a cluster with 559 Fe and 564 Pt atoms is analyzed in Fig. 1. Figure 1(a) shows that at approximately 35 ns, closed packed structures appear, while the amount of icosahedral structure, which is mainly present in the liquidlike state in the surface, decreases. At the same point in time, the temperature of the cluster increases by about 180 K [Fig. 1(b)]. The latent heat of solidification causes this temperature increase. Since the number of collisions with the carrier gas atoms is not sufficient, the solidification heat cannot be removed in the time interval shown here. To calculate the average time $\tau_{\mathrm{gas,cluster}}$ between two collisions of inert gas atoms with the large FePt cluster, we use a formula given by Hendy *et al.*,[38]

$$\tau_{\mathrm{gas,cluster}} \approx \frac{1}{pR^2}\sqrt{\frac{mk_BT}{8\pi}}. \quad (1)$$

Here, R is the cluster radius (1.6 nm), p the pressure of the inert gas, T its temperature (1100 K), m the mass of the inert

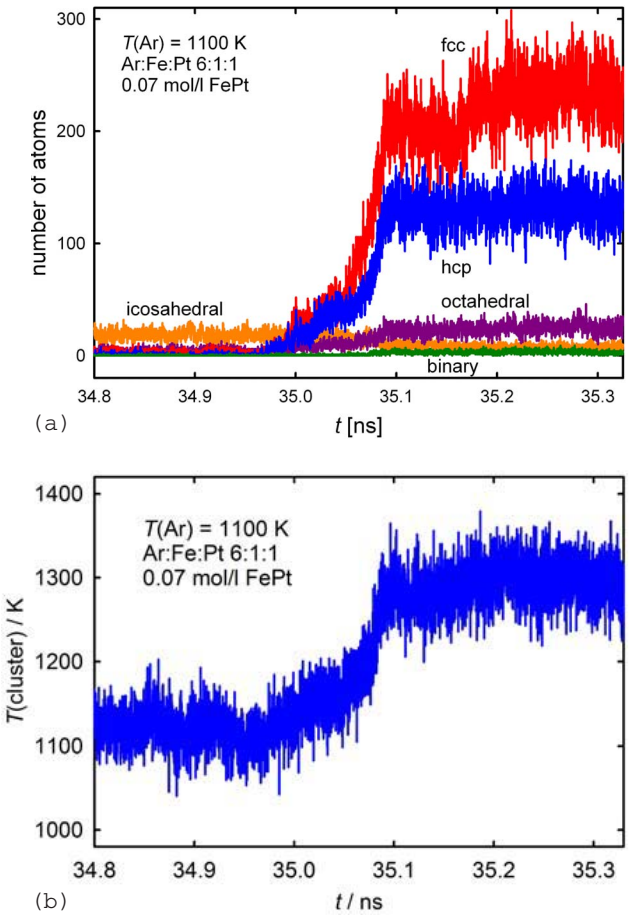

FIG. 1. (Color online) Solidification of a 1123 atom $Fe_{0.5}Pt_{0.5}$ cluster. (a) Structure analysis of the cluster during solidification with the common neighbor analysis (CNA). (b) Cluster temperature during solidification.

gas atoms (argon, 39.948 amu), and k_B the Boltzmann constant. We approximate the pressure p by the ideal gas value and calculate it from the number $N=4116$ of inert gas atoms and the simulation box volume $V=a^3$ with the edge length $a=31.93$ nm. With these assumptions, we get

$$\tau_{\text{gas,cluster}} \approx \frac{a^3}{NR^2}\sqrt{\frac{m}{8\pi k_B T}}, \tag{2}$$

which yields $\tau_{\text{gas,cluster}} \approx 1.3$ ps. It corresponds to 77 collisions within the duration of the solidification process of about 100 ps. This amount of collisions is not sufficient to remove the latent heat from a 1123 atom cluster formed during this time. For the shown time period, the carrier gas temperature is 1100 K. Hence, while energy is removed from the system by the carrier gas, the cluster temperature rises. This corresponds to an apparent negative heat capacity of the system caused by the fact that small cluster solidification is faster than the latent heat removal. In a short time of about 100 ps, the cluster switches completely from the liquidlike state to the solidlike state. In bulk systems with stable static coexistence in equilibrium, the latent heat is taken from the successive solidification of the liquid domain until it is completely solidified. Therefore, the temperature remains constant during solidification and decreases further once the complete system is solid.

Figure 2 shows some snapshots of the solidification process of this cluster. The first snapshot [Fig. 2(a)] represents the liquidlike cluster. There is no structure except for few fluctuations of icosahedral atoms in the surface. In Fig. 2(b), one can observe that a small structured nucleus appears below the surface on the right bottom side of the cluster. This nucleus grows, as one can see in Fig. 2(c), which is 42 ps later than that in Fig. 2(b). During a period of time lasting almost 100 ps, a structured region coexists with a liquidlike region. We do not consider this state as a stable static coexistence because the structured nucleus is continuously growing during this time period. At about 35.09 ns, the cluster rapidly develops structure with exception of the surface layers. A snapshot of the solidlike cluster is shown in Fig. 2(d).

In order to analyze the cluster solidification in detail, we calculate the structure fraction for each shell in the cluster. The structure fraction is defined as the number of atoms in structured environment, obtained from the CNA analysis, related to the total number of atoms. It is calculated here for each shell separately. Moving averages are plotted in Fig. 3(a) for five shells beginning with the surface shell. There are two more shells in the cluster core but they have very few atoms (26 and 3) and therefore exhibit very strong fluctuations of the structure fraction. For this reason, we omit them in the analysis. The outer shell has already some amount of atoms in icosahedral local order in the liquidlike state. All inner shells have no structure before solidification. The offset caused by the icosahedral structure in the liquidlike state in Fig. 3(a) is the reason why the structure fraction of the outer shell crosses the curves for the structure fraction of the inner shells. Besides this effect, one can observe that the structure fraction increases faster for the inner shells than for the outer shells. This is a hint that the cluster nucleates below and not in the surface. One can also recognize that after the transition is completed, the structure fraction decreases from the inner toward the outer shells. Especially, the two most outer shells have a very low structure fraction. The surface layer, for example, has even less than 20% atoms in local order. We do not investigate magic number clusters, so the number of atoms does not match a filled surface shell which leads to defects. Also, the binding energy of the surface atoms is weaker than for the atoms in inner shells, leading to a higher mobility and thus to more disorder. Therefore, we consider the third shell as the first core shell and part of the solidlike region. One can conclude that the cluster solidifies by homogeneous nucleation below the surface layers and in the final state the structure fraction increases toward the cluster center. Plotting only the structure fraction vs time could be misleading since the amount of atoms per shell decreases toward the center of the cluster. The actual number of atoms in local order at the end of the solidification is 80 for the nth shell (most outer), 80 for the $(n-1)$th shell, 110 for the $(n-2)$th shell, 75 for the $(n-3)$th shell, and 40 for the $(n-4)$th shell. The fact that the two outer shells contain most atoms [440 atoms in the nth shell and 280 atoms in the $(n-1)$th shell] also shows that the relatively large amount of structure defects in the overall structure analysis [Fig. 1(a)] is mainly related to the disorder in the surface. Most of the cluster core

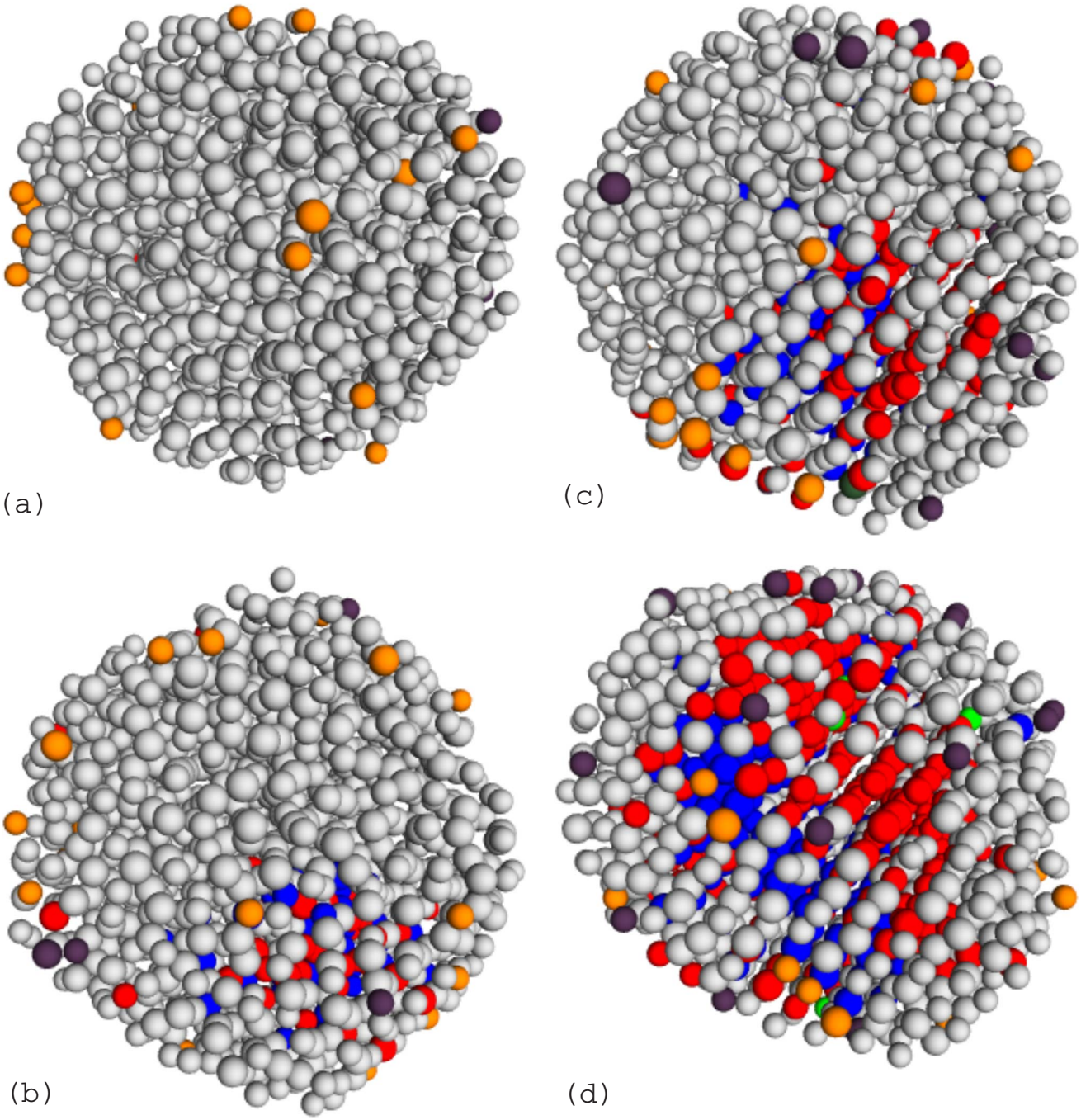

FIG. 2. (Color online) Snapshots during the solidification of the 1123 atom $Fe_{0.5}Pt_{0.5}$ cluster. (a) Liquid state at $t=34.525$ ns. (b) Appearance of a structured nucleus below the surface on the right bottom side of the cluster at $t=35.029$ ns. (c) Like (b) but at $t=35.071$ ns. (d) Completely structured core of the cluster at $t=35.094$ ns. Legend: light gray, atoms without local order; dark gray, atoms with local order (red, fcc; blue, hcp; ochre, icosahedral; violet, octahedral; green, ordered binary face-centered-cubic-like structure).

is structured. Neither the structure fraction nor the total number of atoms in structured environment can clearly distinguish between nucleation in the center of a cluster and right below the two surface layers. However, one can recognize from such a plot that the nucleation starts in the interior of the cluster and not in the surface, which is furthermore supported by the snapshot in Fig. 2(b) where the solid nucleus is clearly visible inside the cluster.

The temperature analysis of the shells does not exhibit any temperature gradient within the cluster during the solidification process. Hence, the thermal equilibration is very fast for the clusters of given size. Therefore, the outer shell does not cool down below the core temperature and the appearance of a solid nucleus is not necessarily more likely in the surface in this context. On the other hand, the atoms in the cluster core below the surface have a higher coordination number than the atoms in the surface. This means that it is energetically more favorable to form the crystal structure inside the cluster than in the cluster surface. Since a temperature difference does not exist, the short range order, coordi-

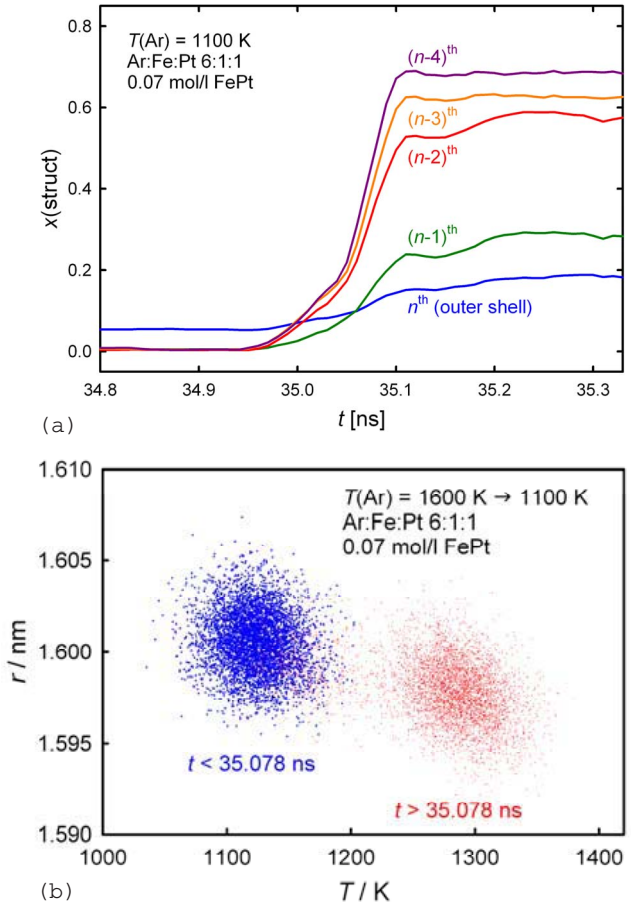

FIG. 3. (Color online) Solidification of the 1123 atom $Fe_{0.5}Pt_{0.5}$ cluster. (a) Moving average of the structure fraction during solidification for each shell separately. (b) Cluster radius plotted against temperature. Blue points are before the onset of solidification ($t < 35.078$ s); the red points after solidification ($t > 35.078$ s).

nation number, and the defects are the only differences between the core and surface. Hence, one possible origin of the solidification below the surface is a local ordering effect.

Another possible origin is that an inhomogeneous composition of the cluster is responsible for the nucleation inside the cluster. Such effect has been pointed out by Chushak and Bartell.[10] We investigate the deviation of the mole fraction of Fe atoms not in local order by the unstructured mole fraction defined as

$$x_{\mathrm{Fe,unstruct}} = \frac{N_{\mathrm{Fe,unstruct}}}{N_{\mathrm{Fe,unstruct}} + N_{\mathrm{Pt,unstruct}}}. \quad (3)$$

This is the ratio of Fe atoms, which are not in local order, to the total number of atoms (Fe and Pt), which are not in local order. Figure 4 shows that the amount of unstructured Fe decreases during solidification. This means that slightly more Fe atoms are in local order than Pt atoms. This can be explained by the fact that the two outer layers, which exhibit much less local order after solidification, are platinum rich (approximately 55% Pt). The cluster core without these two layers is iron rich (approximately 60% Fe). Since the core takes a much higher structure fraction after solidification

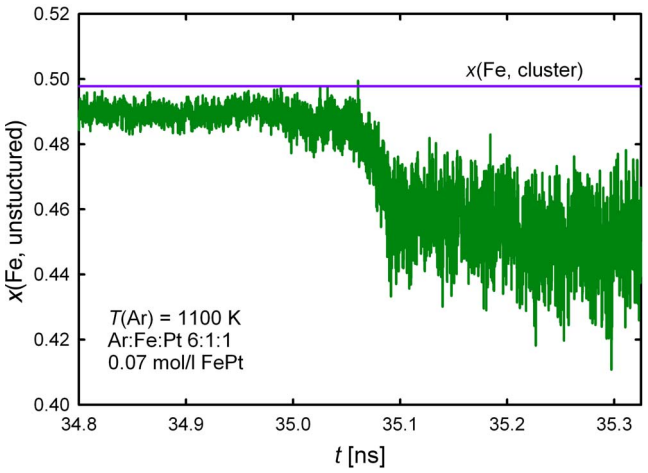

FIG. 4. (Color online) Fraction of iron atoms which are not in local order according to Eq. (3). The horizontal line is the overall iron mole fraction of the complete cluster.

than the surface layers, the fraction of iron atoms without local order decreases slightly during solidification by about 0.04, as one can see in Fig. 4.

We do not find any bcc structure although in bulk solidification, a nucleus can be in bcc structure for a fcc metal because of its lower interfacial energy.[39] On the other hand, it is known that small clusters of a bcc metal can take a fcc structure.[18] This is related to differences in the cluster-vapor surface energy for the two structures. At a temperature above 1100 K, the FePt bulk system is in a face-centered structure for all mole fractions. bcc structure only appears at an iron mole fraction of roughly 0.1 below 900 K, which is far away from the conditions used here. Since we do not find any indications of bcc structure it appears that the effect of the cluster-vapor surface dominates over the solidlike nucleus and liquid interfacial energy in this system.

Figure 3(b) shows that with increasing temperature, the cluster radius and therefore the volume of the cluster decrease. Such negative thermal expansion is counterintuitive but well known for several substances such as water below 4 °C. It should be noted that an invar system such as FePt can exhibit vanishing and negative thermal expansion but only below the Curie temperature of roughly 600 K and only for iron rich systems with at least 65% iron.[40,41] This behavior is therefore not relevant here. Here, the negative thermal expansion is rather related to the fast solidification of the cluster: The cluster radius is related to the atomic ordering which increases at solidification, leading to a higher density or smaller molar volume. Since the cluster heats up during solidification, one obtains increasing density with increasing temperature. In general, the thermal expansion coefficient is proportional to the heat capacity, the compressibility, and the Grüneisen coefficient.[42] With positive compressibility and positive Grüneisen coefficient, only the apparent negative heat capacity can be related to this negative thermal expansion. Hence, this effect can also be regarded as apparent negative thermal expansion. Furthermore, investigations of equimolar FePt clusters over longer simulation time and wide temperature range give positive thermal expansion for

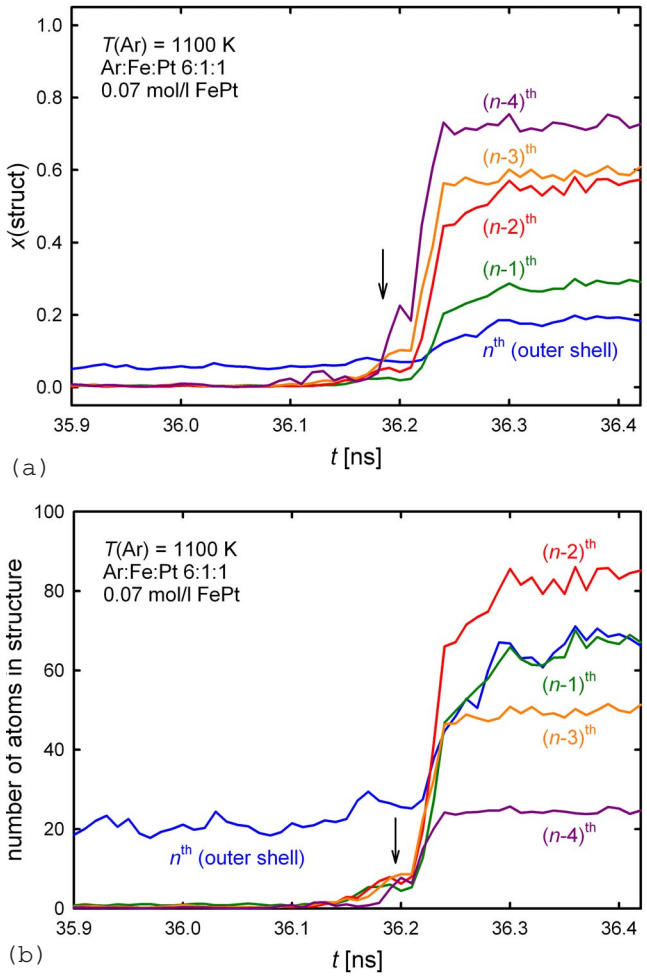

FIG. 5. (Color online) Solidification of an 864 atom $Fe_{0.5}Pt_{0.5}$ cluster. (a) Running average of the structure fraction during solidification for each shell separately. (b) Running average of the total number of atoms in structure corresponding to (a). The arrows mark structure fluctuations prior to nucleation.

both liquidlike and solidlike FePt clusters.[37] It shows that this system, with this composition at a given temperature, does not exhibit negative thermal expansion caused by interactions.

The same investigation is carried out with two smaller clusters consisting of 864 atoms (432 of each Fe and Pt) in the carrier gas argon. While cooling down these clusters from 1600 to 1000 K, the solidification takes place again at a temperature of about 1100 K. Compared to the large cluster, the increase in cluster temperature at the onset of structure formation is a bit smaller (approximately 150 and 110 K). Like in the large cluster, the solidification starts below the surface and moves throughout the cluster in a similar time range (Fig. 5). The fraction of atoms in local order per shell is very similar as for the larger cluster discussed above in detail [Fig. 5(a)]. Figure 5(b) shows the total number of atoms in structured environment. The sequence of the number of structured atoms in the shells is different compared to Fig. 5(a) but regarding the solidification, no significant differences can be deduced. In addition, the 864 atom cluster exhibits some fluctuations of the structure fraction of inner shells prior to nucleation. These stochastic fluctuations, which are characteristic for homogeneous nucleation, are marked by an arrow in Figs. 5(a) and 5(b).

IV. CONCLUSIONS

In summary, we find that FePt clusters with 864 and 1123 atoms solidify quickly for given undercooling within about 100 ps without showing stable static coexistence of liquidlike and solidlike domains. We have observed only cases where nucleation and structure formation took place but no cases where amorphous clusters have been obtained as found for NiAl clusters.[10] A reason for this difference may be the different system studied here but it could also be the 2 orders of magnitude lower cooling rate or the inert gas thermostat employed in our investigation. In agreement with the work on NiAl clusters, we find no and in few cases a small amount of ordered binary structure. This confirms the initial statement concerning the Ostwald step rule. Not the most stable binary ordered $L1_0$ phase appears but the disordered fcc phase. This is in agreement with a recent investigation of the melting of $L1_0$ FePt clusters.[24] When an $L1_0$ cluster is heated up, first the disordered fcc phase forms and only then the cluster melts as indicated by the latent heat.[24] While in this direction from order to disorder the transition is traceable in MD simulations, the binary ordering process in the other direction seems to be beyond the time scale of the MD simulation used so far.

The small FePt clusters equilibrate thermally very rapidly and there is no noticeable temperature gradient in the cluster. In the binary clusters investigated here, nucleation starts below the cluster surface because of the higher degree of local order. In some cases, fluctuations of the shells' structure fraction are observed before the actual nucleation event takes place. It follows that homogeneous nucleation inside the cluster is more likely than heterogeneous nucleation in the cluster surface. With a diameter of around 3 nm, we obtain a solidification velocity of approximately 30 m/s for the clusters. This value is on the order of magnitude of the solidification velocity in bulk systems at comparable degree of undercooling, for example, for CuNi alloys.[43,44] So, if there is no major difference in solidification velocity between bulk and small clusters, the clusters solidify fast simply because of their small size. For the binary clusters investigated here, dynamic coexistence can be regarded as a consequence of small size and incomplete dissipation of heat in a carrier gas compared to a bulk system. It is therefore a kinetic phenomenon in the systems investigated here. This is consequently also the origin of the apparent negative heat capacity and thermal expansion observed here.

ACKNOWLEDGMENT

This work was supported by the Deutsche Forschungsgemeinschaft (DFG) within Project No. Kr 1598/24-2.

[1] D. Gersappe, Phys. Rev. Lett. **89**, 058301 (2002).
[2] Y. H. Lee, G. Lee, J. H. Shim, S. Hwang, J. Kwak, K. Lee, H. Song, and J. T. Park, Chem. Mater. **18**, 4209 (2006).
[3] A. Moser, K. Takano, D. T. Margulies, M. Albrecht, Y. Sonobe, Y. Ikeda, S. Sun, and E. E. Fullerton, J. Phys. D **35**, R157 (2002).
[4] M. Schmidt, R. Kusche, T. Hippler, J. Donges, W. Kronmüller, B. von Issendorff, and H. Haberland, Phys. Rev. Lett. **86**, 1191 (2001).
[5] R. M. Lynden-Bell and D. J. Wales, J. Chem. Phys. **101**, 1460 (1994).
[6] D. J. Wales and R. S. Berry, Phys. Rev. Lett. **73**, 2875 (1994).
[7] J. A. Reyes-Nava, I. L. Garzón, and K. Michaelian, Phys. Rev. B **67**, 165401 (2003).
[8] W. Zhin-Min, W. Xin-Quiang, and Y. Yuan-Yuan, Chin. Phys. **16**, 1009 (2007).
[9] K. vF. MacDonald, F. Soares, V. Bashevoy, and N. I. Zheludev, IEEE J. Sel. Top. Quantum Electron. **12**, 371 (2006).
[10] Y. G. Chushak and L. S. Bartell, J. Phys. Chem. B **107**, 3747 (2003).
[11] E. Mendez-Villuendas and R. K. Bowles, Phys. Rev. Lett. **98**, 185503 (2007).
[12] J. G. Lee and H. Mori, Phys. Rev. B **70**, 144105 (2004).
[13] S. Pochon, K. F. Mac Donald, R. J. Knize, and N. I. Zheludev, Phys. Rev. Lett. **92**, 145702 (2004).
[14] D. Schebarchov and S. C. Hendy, Phys. Rev. Lett. **96**, 256101 (2006).
[15] O. H. Nielsen, J. P. Sethna, P. Stoltze, K. W. Jacobsen, and J. K. Norskov, Europhys. Lett. **26**, 51 (1994).
[16] S. C. Hendy, Phys. Rev. B **71**, 115404 (2005).
[17] P. Erhart and K. Albe, Appl. Surf. Sci. **226**, 12 (2004).
[18] N. Lümmen and T. Kraska, Nanotechnology **15**, 525 (2004).
[19] S. Sun, C. B. Murray, D. Weller, L. Folks, and A. Moser, Science **287**, 1989 (2000).
[20] N. Lümmen and T. Kraska, Eur. Phys. J. D **41**, 247 (2007).
[21] N. Lümmen and T. Kraska, Phys. Rev. B **71**, 205403 (2005).
[22] M. S. Daw and M. I. Baskes, Phys. Rev. Lett. **50**, 1285 (1983).
[23] R. Meyer and P. Entel, Phys. Rev. B **57**, 5140 (1998).
[24] N. Lümmen and T. Kraska, Modell. Simul. Mater. Sci. Eng. **15**, 319 (2007).
[25] Y. Chen, S. Iwata, and T. Mohri, CALPHAD: Comput. Coupling Phase Diagrams Thermochem. **26**, 583 (2002).
[26] W. Ostwald, Z. Phys. Chem., Stoechiom. Verwandtschaftsl. **22**, 289 (1897).
[27] P. Fredriksson and B. Sundman, CALPHAD: Comput. Coupling Phase Diagrams Thermochem. **25**, 535 (2001).
[28] J. D. Honeycutt and A. C. Andersen, J. Phys. Chem. **91**, 4950 (1987).
[29] A. S. Clarke and H. Jónsson, Phys. Rev. E **47**, 3975 (1993).
[30] D. Faken and H. Jónsson, Comput. Mater. Sci. **2**, 279 (1994).
[31] C. L. Cleveland, W. D. Luedtke, and U. Landman, Phys. Rev. Lett. **81**, 2036 (1998).
[32] Y. Wang, S. Teitel, and C. Dellago, J. Chem. Phys. **122**, 214722 (2005).
[33] *Binary Phase Diagrams*, edited by T. B. Massalski, J. L. Murray, L. H. Bennet, and H. Baker (ASM International, Materials Park, OH, 1986), p. 1096.
[34] M. Hausen and K. Anderko, *Constitution of Binary Alloys* (McGraw-Hill, New York, 1958).
[35] Y. K. Takahashi, T. Ohkubo, M. Ohnuma, and K. Hono, J. Appl. Phys. **93**, 7166 (2003).
[36] T. Schenk, D. Holland-Moritz, and D. M. Herlach, Europhys. Lett. **50**, 402 (2000).
[37] R. Rozas, N. Lümmen, and T. Kraska, Eur. Phys. J. Spec. Top. **149**, 57 (2007).
[38] S. Hendy, S. A. Brown, and M. Hyslop, Phys. Rev. B **68**, 241403(R) (2003).
[39] F. Spaepen and R. B. Meyer, Scr. Metall. **10**, 257 (1976).
[40] B. Rellinghaus, J. Kästner, T. Schneider, E. F. Wassermann, and P. Mohn, Phys. Rev. B **51**, 2983 (1995).
[41] S. Khmelevskyi, I. Turek, and P. Mohn, Phys. Rev. Lett. **91**, 037201 (2003).
[42] G. D. Barrera, J. A. O. Bruno, T. H. K. Baron, and N. L. Allan, J. Phys.: Condens. Matter **17**, R217 (2005).
[43] R. Willnecker, D. M. Herlach, and B. Feuerbacher, Phys. Rev. Lett. **62**, 2707 (1989).
[44] P. R. Algoso, W. H. Hofmeister, and R. J. Bayuzik, Acta Mater. **51**, 4307 (2003).